Iranian Journal of Hydrogen & Fuel Cell 4(2015) 215-226

Iranian Journal of Hydrogen & Fuel Cell

IJHFC

Journal homepage://ijhfc.irost.ir

Effect of K_2O on the catalytic performance of Ni catalysts supported on nanocrystalline Al_2O_3 in CO_2 reforming of methane

Zahra Alipour[1], Fereshteh Meshkani[1], Mehran Rezaei[1,2,*]

[1] Catalyst and Advanced Materials Research Laboratory, Chemical Engineering Department, Faculty of Engineering, University of Kashan, Kashan, Iran

[2] Institute of Nanoscience and Nanotechnology, University of Kashan, Kashan, Iran

Article Information

Article History:

Received:
14 December 2015
Received in revised form:
09 March 2016
Accepted:
12 April 2016

Keywords

Nickel catalyst
Promoters
Potassium
CO_2 reforming

Abstract

CO_2 reforming of methane (CRM) over unpromoted and potassium promoted Ni/Al_2O_3 catalysts was studied. The catalysts were prepared by the impregnation method and characterized by X-ray diffraction (XRD), N_2 adsorption (BET), temperature programmed reduction (TPR), temperature programmed oxidation (TPO) and scanning electron microscope (SEM) techniques. The obtained results showed that addition of K_2O to the Ni/Al_2O_3 catalyst increased surface area. Also, the addition of K_2O to this catalyst increased activity and decreased the amount of deposited carbon by enhancing the basic properties of the catalysts and CO_2 adsorption and preventing the Boudouard reaction. In addition, the effect of Ni and potassium loadings were investigated in Ni/K_2O-Al_2O_3 catalysts. It was observed that by increasing nickel content, the specific surface area decreased, but catalytic activity and coke formation increased. Also, catalytic tests showed that just a moderate amount of K could improve catalytic activity and decrease coke formation in the Ni/K_2O-Al_2O_3 catalyst in dry reforming of methane.

1. Introduction

In the last years, the CO_2 reforming of methane (1) has attracted increasing interest as it is a reaction that produces synthesis gas with a H_2/CO ratio close to unity, and contributes to the removal of methane and carbon dioxide, the two most important green-house gases [1-7].

$$CH_4 + CO_2 \rightarrow 2H_2 + 2CO \quad (1)$$

However, deactivation of the catalyst creates difficulties for its application in the industrial level due to coke accumulation and sintering of both support and active metal particles [8-10]. Various catalysts have been developed for this reaction. Noble metals

*Corresponding Author's E-mail address: rezaei@kashanu.ac.ir

such as Pt, Rh, and Pd are reported to be active and fairly stable for the CO_2 reforming of CH_4. However, they are too expensive to utilize practically. Inexpensive transition metals such as Fe, Co, and Ni are also known to be active for the reaction to some extent, and among these Ni is the most favorable. The Ni-based catalysts have high activity and selectivity, but the major drawback of this reaction is the rapid deactivation of the catalysts as a result of carbon deposition. The origin of inactive carbon, C(s), during CO_2 reforming of methane may occur either via CH_4 decomposition ($CH_4 \rightarrow C+ 2H_2$) and/or the Boudouard reaction ($2CO \rightarrow C+ CO_2$) [8, 11-17].

The amount of deposited carbon can be affected by the nature of the support, the preparation method and the addition of promoters. Among the promoters, the alkali metal oxides (K_2O, Cs_2O, etc.) and alkaline earth metal oxides (MgO, CaO, BaO, etc.) are commonly chosen as support modifiers or promoters [16, 18-19]. The main objective of the present study was to investigate the effects of potassium oxide as a promoter for the Ni/Al_2O_3 catalyst in the dry reforming reaction. In addition, the effects of nickel and potassium contents were studied on the textural and catalytic performance.

2. Experimental

2.1. Catalyst preparation

The catalysts employed in the present work were prepared by the wet impregnation method. Nickel nitrate ($NiN_2O_6.6H_2O$) and KNO_2 were used as Ni and K precursors, respectively. γ–Al_2O_3, as catalyst support, was prepared by the sol-gel method. For this purpose, aluminum tri isopropylate (98% purity, Merck) was first hydrolyzed in distillated water by stirring for 1 hour at 80-85˚C. Subsequently, HNO_3 was added dropwise with an HNO_3 to Al molar ratio of 1:1 and refluxed for 12h at 98˚C. Then, the sol was kept for 2h at 98ºC in air. After this step the sol became very viscous. The formed gel was dried overnight at 80˚C and calcined at 600˚C for 4h. Next, the prepared γ –Al_2O_3 was impregnated with an aqueous solution of potassium salt with an appropriate concentration to obtain the desired content of potassium. After impregnation the promoted support was dried at 80˚C overnight and calcined at 700˚C for 4h. The promoted γ–Al_2O_3 was then impregnated with nickel nitrate with an appropriate concentration to get the desired content of nickel. Finally, the impregnated samples were dried at 80˚C overnight and calcined at 500˚C for 4h.

2.2. Characterization

The N_2 adsorption/desorption analysis was carried out at boiling temperature of nitrogen (−196˚C) using an automated gas adsorption analyzer (Tristar 3020, Micromeritics). The samples were purged with nitrogen gas for 2h at 200˚C using a VacPrep 061 degas system (Micromeritics). Temperature programmed reduction (TPR) analysis was used for evaluating the reduction properties of the prepared catalysts with Micromeritics chemisorb 2750 gas-adsorption equipment. In the TPR measurement, 200 mg of catalyst was subjected to a heat treatment (10˚C/min) in a gas flow (30 ml/min) containing a mixture of H_2: Ar (10:90). Prior to the TPR experiment, the samples were heat treated under an inert atmosphere (Ar) at 200ºC for 2h. The H_2 uptake amount during the reduction was measured using a thermal conductivity detector (TCD). Temperature-programmed oxidation (TPO) of the spent catalysts was carried out using a similar apparatus by introducing a gas flow (30 mL/min) containing a mixture of O_2: He (5:95) and the temperature was increased up to 800˚C at a heating rate of 10˚C/min. Scanning electron microscopy (SEM) analysis was performed with VEGA TESCAN operated at 30 kV.

2.3. Catalytic activity measurement

The catalytic activity measurements were carried out in a tubular fixed-bed continuous-flow reactor made of quartz (i.d. 8 mm) under atmospheric pressure. To control the catalyst bed temperature the thermocouple was introduced at the bottom of the catalyst bed.

The reactor was loaded with 200 mg of the prepared catalyst. Prior to the reaction, the catalysts were reduced in a H_2 gas flow of 20 mL.min^{-1} at 600˚C for 2h. The reactant gas feed, consisting of CH_4 and CO_2, was introduced into the reactor and the activity tests were performed at different temperatures, ranging from 550 to 700˚C in steps of 50˚C. The flow rates were controlled by Bronkhorst High-Tech mass flow meter/controllers EL-FLOW® Select Series. The loss in catalyst activity at 700˚C was monitored up to a 5h time on stream. The gas composition of reactants and products were analyzed using a gas chromatograph (Varian 3400) equipped with a TCD and a Carboxen 1000 column.

3. Results and discussion

3.1. Structural properties of the catalysts

Physicochemical properties of the catalysts are summarized in Table 1. It is seen that all the samples possessed high specific surface areas up to 162 m^2.g^{-1}. The average pore diameters of the samples were located in the range of 8.3-8.6 nm, which belong to mesoporous materials according to the definition of the IUPAC (2-50 nm) [5]. It is seen that the addition of a potassium promoter to the 5%Ni/Al_2O_3 catalysts decreased the S_{BET} and pore volume due to the blocking of some pores of support by potassium. Likewise, particle size increased with the addition of a potassium promoter.

Figures 1a and b show the nitrogen adsorption/desorption isotherms and pore size distributions of the prepared catalysts, respectively. For both samples, the isotherms can be classified as a type IV isotherm, typical of mesoporous materials. According to IUPAC classification, the hysteresis loop is type H2. In this case pores can have non uniform size or shape [20]. As it is shown in Figure 1b, the pore size distributions of these catalysts are located between 5-17 nm.

The XRD pattern of unpromoted 5wt.% Ni/Al_2O_3 catalysts is shown in Figure 2. As shown in this figure, the observed peaks at 2θ = 37.2° and 45.9° are assigned

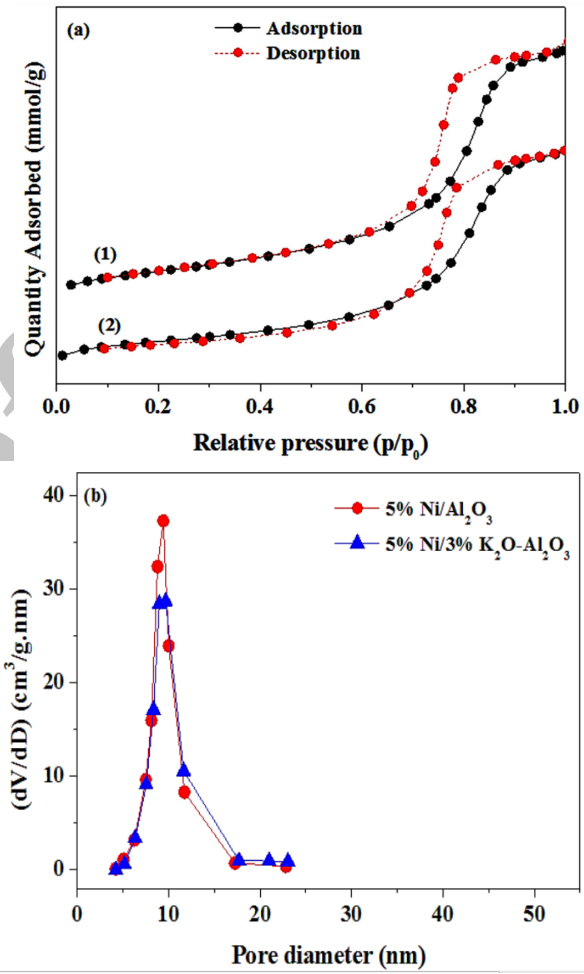

Fig. 1. (a) N_2 adsorption/desorption isotherms and (b) pore size distributions of calcined catalysts.

to Al_2O_3 (JCPDS Card No. 01-1303). The peak at about 2θ = 62° is ascribed to the $NiAl_2O_4$ phase

Table 1. Structural properties of the catalysts

Catalyst	S_{BET} ($m^2.g^{-1}$)	Pore volume ($cm^3.g^{-1}$)	Pore width (nm)	Particle Size[a] (nm)
5%Ni/Al_2O_3	173	0.52	8.37	8.20
5%Ni/3%K_2O-Al_2O_3	162	0.46	8.62	8.86

[a] calculated by D=6000/(S_{BET}. density)

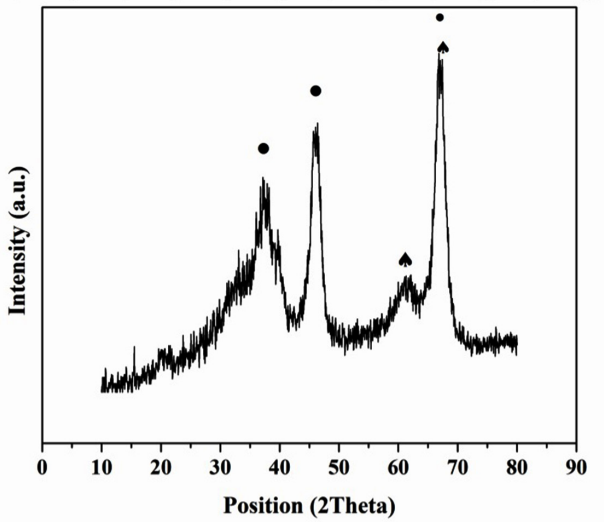

Fig. 2. The XRD pattern of 5wt.%Ni/Al_2O_3. (•) Al_2O_3, (♠) $NiAl_2O_4$.

(JCPDS Card No. 71-0963). The Al_2O_3 and $NiAl_2O_4$ phases are overlapped at 2θ = 67°. Moreover, the diffraction peaks of the NiO phase were not detected in this catalyst due to the high dispersion of NiO on the support. For the promoted catalysts the diffraction peaks (not shown here) related to K_2O were probably not detected because of the low percentage of this promoter, which is in agreement with other published results [2, 21-22].

3.2. Temperature- programmed reduction (TPR)

TPR profiles of Ni/γ-Al_2O_3 and K_2O promoted catalysts are displayed in Figure 3. The unpromoted catalyst showed two main reduction peaks in the TPR profile, while the K_2O promoted catalyst exhibited three main reduction peaks. The extra peak at 500˚C in the promoted catalyst is attributed to NiO species with weak interaction with the catalyst support. In both catalysts, the first broad peak observed between 600-700˚C can be ascribed to the reduction of NiO species with strong interaction with support. The second peak between 800-900˚C is assigned to the reduction of $NiAl_2O_4$. This corresponds with other literature [19, 21-22]. It is obvious that by adding K_2O to the catalyst, the reduction temperature was shifted lower, which led to an improvement in catalyst reducibility.

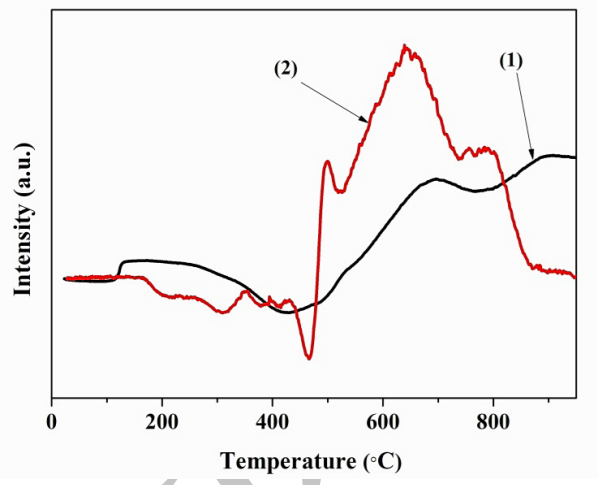

Fig. 3. TPR patterns of (1) 5%Ni/Al_2O_3, (2) 5%Ni/3%K_2O/Al_2O_3 catalysts.

3.3. Catalytic performance

The conversions of CH_4 and CO_2 are shown in Figure 4a and b, respectively. The results showed that with increasing reaction temperature, the conversions of CO_2 and CH_4 increased from 550-700˚C due to the endothermic character of the CRM reaction. It is also obvious that the conversion of CO_2 is higher than that of CH_4 on the unpromoted and promoted catalysts due to the reverse water-gas shift reaction ($CO_2 + H_2 \leftrightarrow CO + H_2O$). As can be seen in Figure 4a and b, K_2O significantly improved the catalytic activity [23].

The H_2/CO molar ratios on both catalysts are displayed in Figure 4c. It is clear that the H_2 /CO molar ratio for both catalysts is less than one because of the occurrence of the reverse water gas shift reaction. Meanwhile, by increasing the temperature, the endothermic dry reforming reaction proceeds better and hence the H_2/CO ratio increases.

A short time stability test was carried out at 700˚C and the results showed that both the catalysts exhibited high stability during the test period of 300 min (Figure 5).

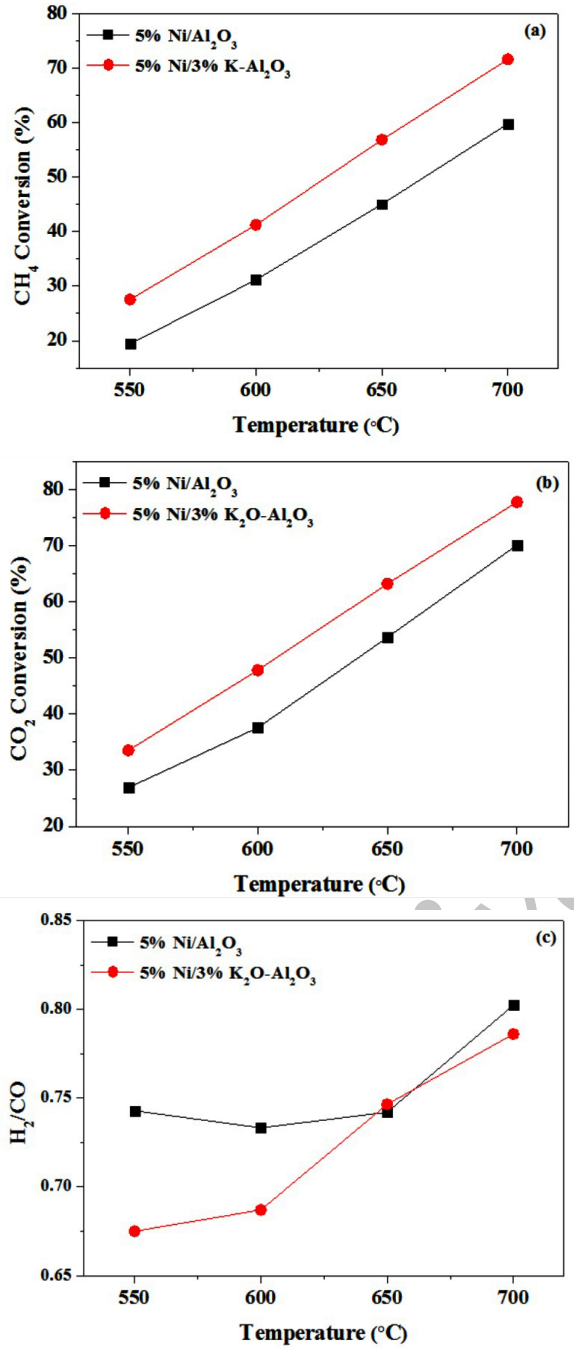

Fig. 4. (a) CH_4 conversion, (b) CO_2 conversion and (c) H_2/CO ratio. Reaction conditions: CH_4/CO_2=1/1, GHSV = 12000 (ml/h.g_{cat}).

3.4. Coke formation

3.4.1. Temperature- programmed oxidation (TPO)

Figure 6 shows the TPO profiles of the spent Ni/Al_2O_3 and $Ni/K\text{-}Al_2O_3$ catalysts. Three peaks appearing in the TPO profile of the unpromoted catalyst are attributed to different types of deposited carbon. They can be categorized as active carbon species or reaction intermediates that reacted with oxygen at low temperatures, amorphous and/or graphite forms of carbon and filamentous carbon, respectively. As can be seen, the addition of a potassium promoter to the Ni/Al_2O_3 catalyst decreased the amount of deposited carbon. The decrease in carbon formation is related to the enhancement of the basic properties of the catalysts and consequently increases the CO_2 adsorption capacity on the catalysts, which inhibits the CO decomposition reaction ($2CO \leftrightarrow C + CO_2$) and suppresses the coke formation [14].

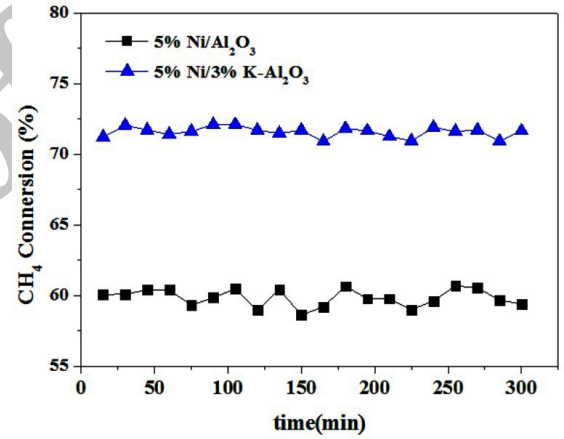

Fig. 5. Short time stability of the Ni/Al_2O_3, $Ni/K\text{-}Al_2O_3$ catalysts. Reaction condition: T= 700°C, CH_4:CO_2= 1/1, GHSV= 12000(ml/h.g_{cat}).

3.4.2. SEM analysis

Figure 7a and b shows the SEM images of the spent Ni/Al_2O_3 and promoted nickel catalysts, respectively. As can be seen, catalyst filamentous carbon was observed in the Ni/Al_2O_3, but no deposited carbon was observed in the potassium promoted catalyst. The SEM results showed that the addition of a K_2O promoter significantly decreased the amount of deposited carbon. These results are in agreement with those observed from the TPO analysis.

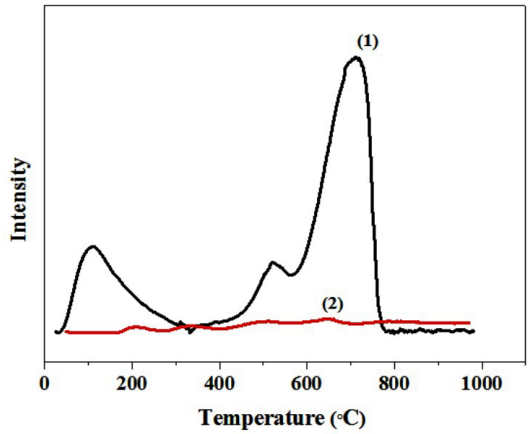

Fig. 6. TPO profiles of the spent (1) Ni/Al_2O_3 and (2) $Ni/K\text{-}Al_2O_3$ catalysts

3.5. Effect of nickel loading

3.5.1. Structural properties of the catalysts

The structural properties of the $Ni/K_2O\text{-}Al_2O_3$ catalysts with different Ni loadings are summarized in Table 2. As can be seen, when the Ni loading increased S_{BET}, pore volume and pore diameter decreased but the particle size increased. Figure 8a displays the nitrogen adsorption/desorption isotherms of these catalysts. All the samples showed a IV type isotherm with a H2 shaped hysteresis loop, which indicated mesoporous features. The H2 shaped hysteresis loops also illuminated that all the mesopores were cylindrical-shaped channels with non-uniform pores [20]. The pore size distributions of these samples are presented in Figure 8b. It could be observed that the position of the peaks were located in the range of 5–17 nm.

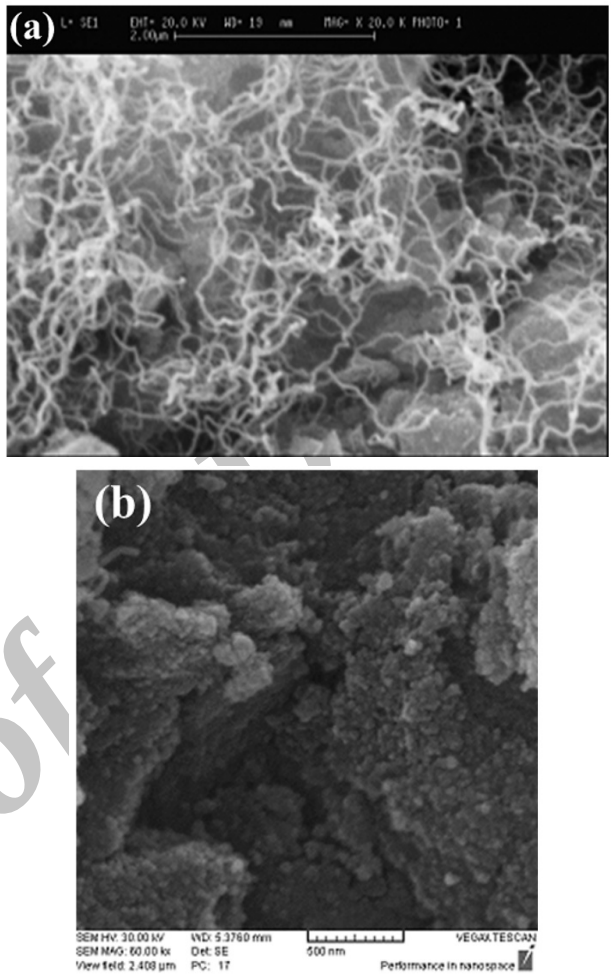

Fig. 7. SEM images of the spent (a) Ni/Al_2O_3, (b) $Ni/K\text{-}Al_2O_3$ catalysts. Reaction conditions: CH_4/CO_2=1, GHSV=12000 ml/g.h, time on the stream=300min.

3.5.2. Temperature- programmed reduction (TPR)

Figure 9 displays the TPR profiles of the fresh $Ni/K_2O\text{-}Al_2O_3$ catalysts with different nickel contents. Three reduction peaks were observed in the TPR profile

Table 2. Structural properties of the $Ni/K_2O\text{-}Al_2O_3$ catalysts with different nickel loadings

Catalyst	S_{BET} ($m^2.g^{-1}$)	Pore volume ($cm^3.g^{-1}$)	Pore width (nm)	Particle Size[a] (nm)
$5\%Ni/3\%K_2O\text{-}Al_2O_3$	162	0.46	8.63	8.86
$10\%Ni/3\%K_2O\text{-}Al_2O_3$	143	0.43	8.59	9.74
$15\%Ni/3\%K_2O\text{-}Al_2O_3$	131	0.39	8.62	10.33
$20\%Ni/3\%K_2O\text{-}Al_2O_3$	120	0.34	8.36	10.96

[a] calculated by $D=6000/(S_{BET}.\ density)$.

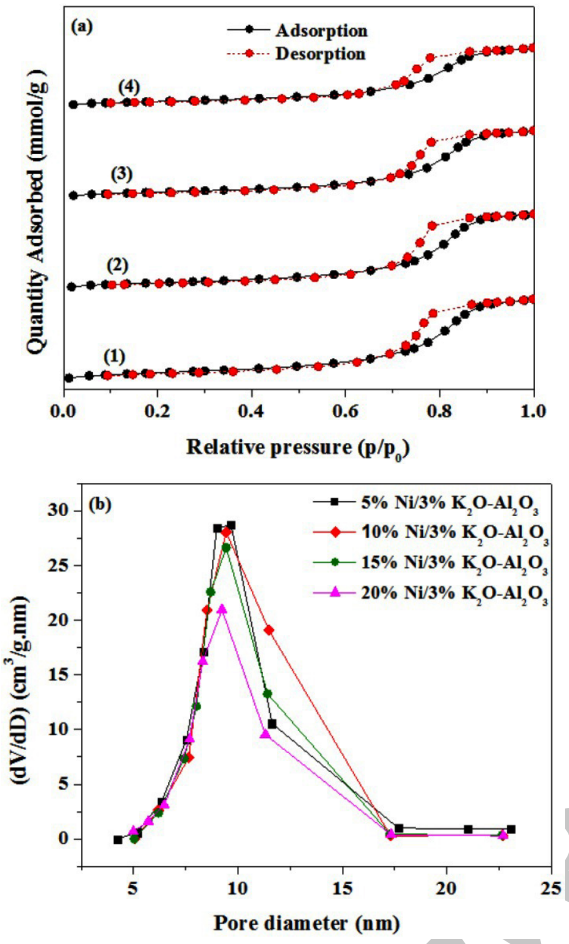

Fig. 8. (a) N_2 adsorption/desorption isotherms (b) and pore size distributions of the calcined catalysts.

of the catalysts with 5% and 10 wt% Ni. These peaks are assigned to NiO species with weak interaction with the support, NiO species with high interaction with the catalyst support and $NiAl_2O_4$ species, respectively. Four reduction peaks were detected in the catalysts with 15% and 20 wt% Ni. The first peak at 450-500˚C is related to free NiO, the second one at 550-600˚C is ascribed to NiO phases with weak interaction with the support, the third one at about 700˚C is attributed to NiO species with high interaction with the catalyst support and the last low intensity peak is assigned to the reduction of $NiAl_2O_4$. As can be seen, as the Ni loading increased, the reduction temperature shifted to lower temperatures. It can be concluded that increases in Ni content increased the content of bulk NiO on the catalyst support and decreased the metal support interaction, which led to an improvement in reducibility of the catalysts.

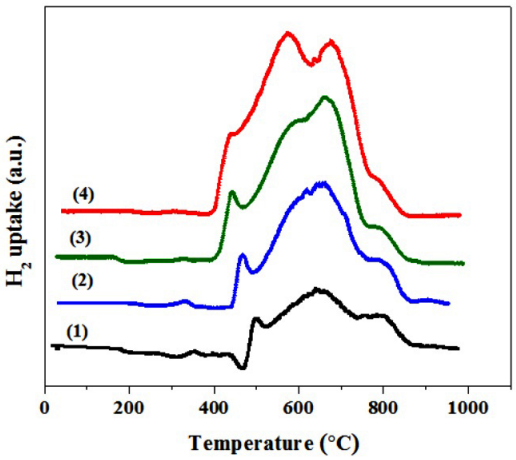

Fig. 9. TPR patterns of the Ni/K_2O-Al_2O_3 catalysts with different Ni loadings. (1) 5%Ni/3%K_2O-Al_2O_3, (2) 10%Ni/3%K_2O-Al_2O_3, (3) 15%Ni/3%K_2O-Al_2O_3, (4) 20%Ni/3%K_2O-Al_2O_3.

3.5.3. Catalytic activity

The reactant conversion and H_2/CO ratio obtained for Ni/K-Al_2O_3 catalysts with different Ni loadings are shown in Figure 10a and b. It is seen that increases in the reaction temperature increased the conversions of CO_2 and CH_4 due to the endothermic nature of the CRM reaction. It is also obvious that the conversion of CO_2 is higher than that of CH_4 due to the reverse water-gas shift reaction ($CO_2 + H_2 \leftrightarrow CO + H_2O$). It was found that the conversion of CH_4 and CO_2 increased as the Ni loading increased from 5% to 20 wt.%, suggesting that more active sites were provided with the increase in Ni loading.

3.5.4. Temperature programmed oxidation(TPO)

Figure 11 shows the temperature programmed oxidation of the spent Ni/K-Al_2O_3 catalysts with different nickel loadings. It is seen that only one oxidation peak was detected for all the catalysts, corresponding to the filamentous carbon [24]. Theobtained results showed that with an increase in Ni loading the intensity of the peak in these profiles increased because of an increase in the amount of deposited carbon. The highest amount of coke deposition was observed over the 20wt%Ni/3wt%K-Al_2O_3 catalyst. The increase in the

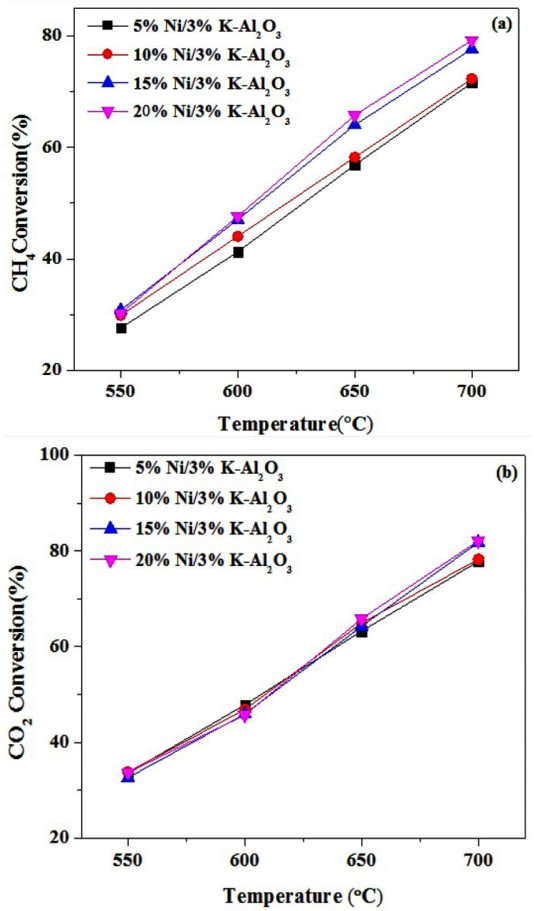

Fig. 10. (a) CH_4 conversion, (b) CO_2 conversion and (c) H_2/CO ratio. Reaction conditions: CH_4/CO_2=1:1, GHSV= 12000 (ml/h.g_{cat}).

coke deposition on the catalysts with higher nickel loadings could be related to the larger particle size and lower Ni dispersion [25].

3.5.5. SEM analysis

The SEM images of the spent 5%Ni/3%K-Al_2O_3 and 15%Ni/3%K-Al_2O_3 catalysts are shown in Figure 12a and b, respectively. As can be seen, the filamentous carbon formation is increased whe the Ni loading increased from 5 to 15 wt.% due to lower dispersion of nickel in 15%Ni/3%K-Al_2O_3 compared with 5%Ni/3%K-Al_2O_3 catalyst. This is in agreement with TPO results.

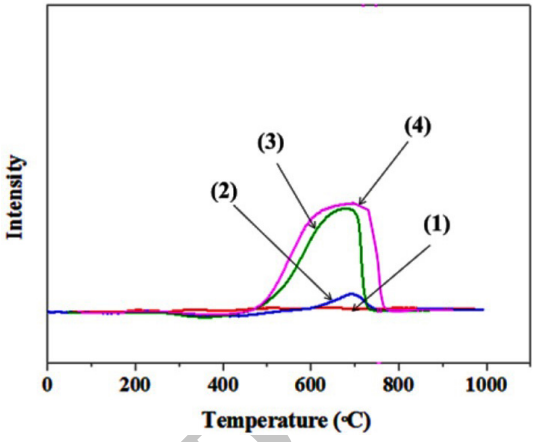

Fig. 11. TPO analysis of the Ni/K-Al_2O_3 with different Ni loadings. (1) 5%Ni/3%K-Al_2O_3, (2) 10%Ni/3%K-Al_2O_3, (3) 15%Ni/3%K-Al_2O_3, (4) 20%Ni/3%K-Al_2O_3.

3.6. Effect of potassium loading

3.6.1. Structural properties of the catalysts

The specific surface area (BET surface area), pore size and pore volume of the 15%Ni/K_2O-Al_2O_3 catalysts with different potassium loadings are listed in Table 3. It is obvious that the addition of 1.5 and 3 wt.% K_2O to the nickel catalyst does not have a significant effect on the BET surface area and pore volume. However, further increase in K_2O content decreased the BET area and pore volume due to pore filling with potassium. The same trend was also observed for the particle size as indicated in Table 3.

The N_2 adsorption/desorption isotherm of the prepared samples are shown in Figure 13a. All the prepared catalysts exhibited the IV type isotherm with a H2 shaped hysteresis loop, which are the significant features for mesoporous materials. Furthermore, the pore size distributions of these materials are shown in Figure 13b. The pore size distributions are located in the range of 5–20 nm.

3.6.2. Temperature- programmed reduction (TPR)

TPR profiles of the Ni/K_2O-Al_2O_3 catalysts with different potassium loadings are presented in

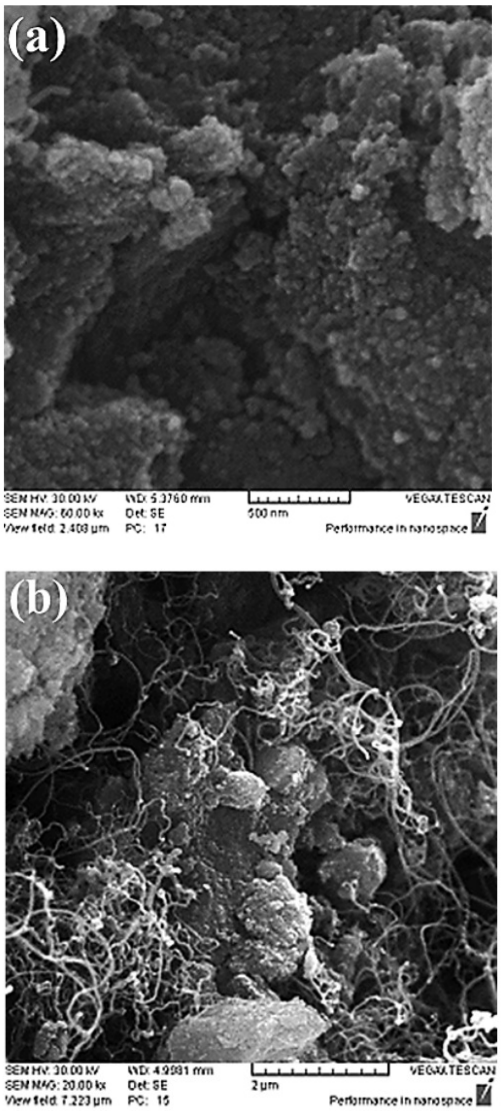

Fig. 12. SEM images of (a) 5%Ni/3%K-Al_2O_3 and (b) 15%Ni/3%K-Al_2O_3 catalysts. Reaction conditions: CH_4/ CO_2=1, GHSV=12000 ml/g.h, time on the stream=300min.

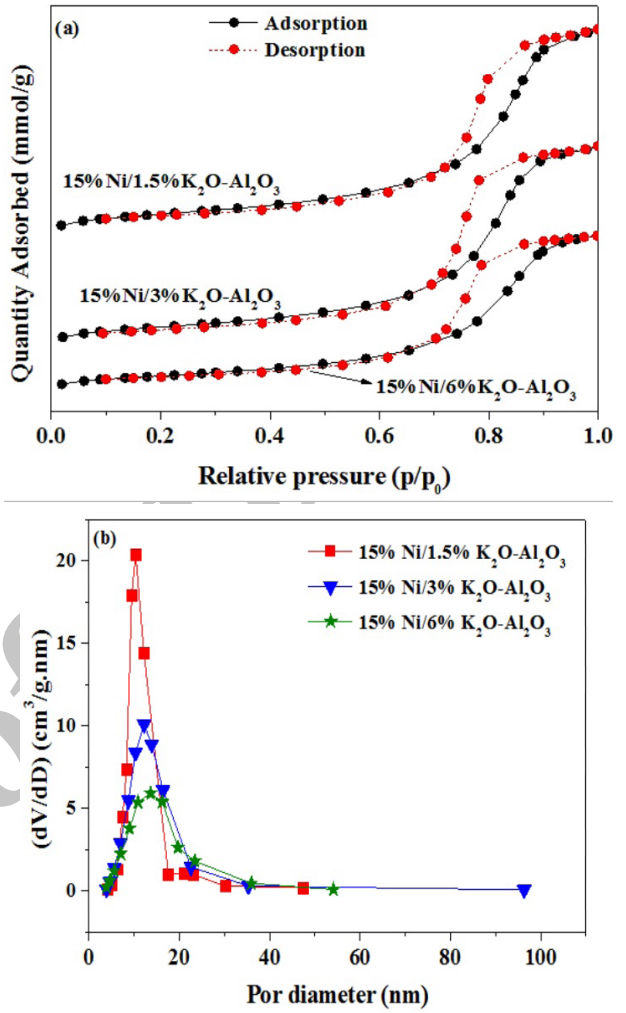

Fig. 13. (a) N_2 adsorption/desorption isotherms and (b) pore size distributions of the Ni/K_2O-Al_2O_3 catalysts with different potassium contents.

Figure 14. It is seen that for all the samples four reduction peaks were detected. The first peak at about 400-450˚C is attributed to the bulk NiO. The second peak located at 600˚C is ascribed to the reduction of NiO species with weak interaction with the support. The third one is related to the NiO species with strong interaction with the catalyst support and the last small peak at about 850˚C is assigned to the reduction of $NiAl_2O_4$. It is seen that the reduction temperature was shifted to higher temperatures by increasing potassium content. The results revealed that the reducibility of the catalysts decreased with the increase in potassium content.

3.6.3. Catalytic performance

Figure 15 shows the catalytic performance of Ni/K-Al_2O_3 catalysts with different potassium loadings. As can be seen, CH_4 and CO_2 conversions increased when the reaction temperature increased from 550 to 700˚C, due to the intensely endothermic character of the CRM reaction [5]. It is also obvious that CO_2 conversion is higher than CH_4 conversion due to the reverse water- gas shift reaction ($CO_2 + H_2 \leftrightarrow CO + H_2O$). It is found that by increasing

Table. 3. Structural properties of the Ni/K_2O-Al_2O_3 catalysts with different potassium loadings

Catalyst	S_{BET} ($m^2.g^{-1}$)	Pore volume ($cm^3.g^{-1}$)	Pore width (nm)	Particle Size[a] (nm)
15%Ni/1.5%K_2O-Al_2O_3	132	0.38	9.42	10.19
15%Ni/3%K_2O-Al_2O_3	131	0.39	8.62	10.33
15%Ni/6%K_2O-Al_2O_3	117	0.30	8.66	11.70

[a] calculated by D=6000/(S_{BET}. density)

the potassium content from 1.5% to 3 wt.%, CH_4 and CO_2 conversions increased. However, further increase in potassium content to 6 .%, decreased the catalytic activity. This confirms that there is an optimum for potassium content in which the catalyst showed the highest catalytic activity and the lowest carbon deposition. Although an increase in potassium content increased the basicity of the catalyst, which can improve the resistance of the catalyst against carbon formation, it can reduce the catalytic activity when the content of potassium increased above the optimum content. The addition of potassium above than the optimum content can reduce the BET surface area and nickel dispersion and consequently decrease the catalytic activity.

3.6.4. Temperature- programmed oxidation (TPO)

Temperature- programmed oxidation (TPO) analysis were carried out on the spent Ni/K-Al_2O_3 catalysts

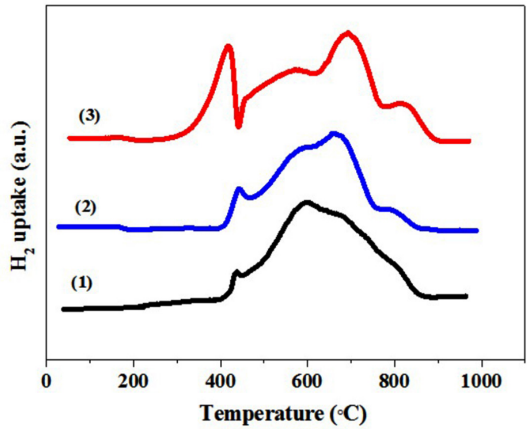

Fig. 14. TPR patterns of (1) 15%Ni/1.5%K_2O-Al_2O_3, (2) 15%Ni/3%K_2O-Al_2O_3, (3) 15%Ni/6%K_2O-Al_2O_3, catalysts.

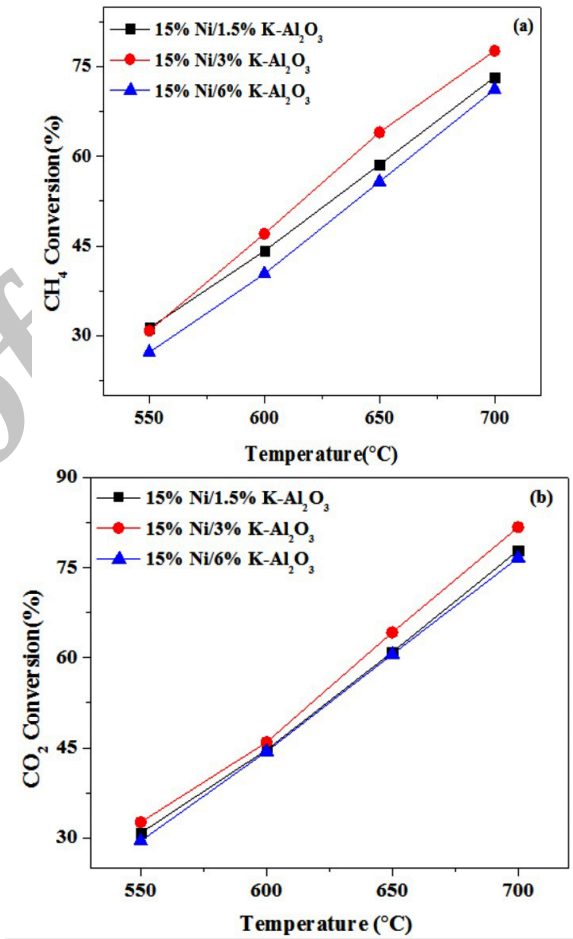

Fig. 15. (a) CH_4 conversion, (b) CO_2 conversion. Reaction conditions: CH_4/CO_2=1/1, GHSV=12000(ml/h.g_{cat}).

with different potassium loadings (Figure 16). The results showed just one peak, which is related to the whisker type carbon detected in all the samples. As can be seen, the highest and the lowest amount of deposited coke were detected in the catalysts with 3% and 6% potassium, respectively. It is worth noting that 15%Ni/3%K-Al_2O_3 and 15%Ni/1.5%K-Al_2O_3 catalysts exhibited the highest and the lowest catalytic

activity among the studied samples, respectively.

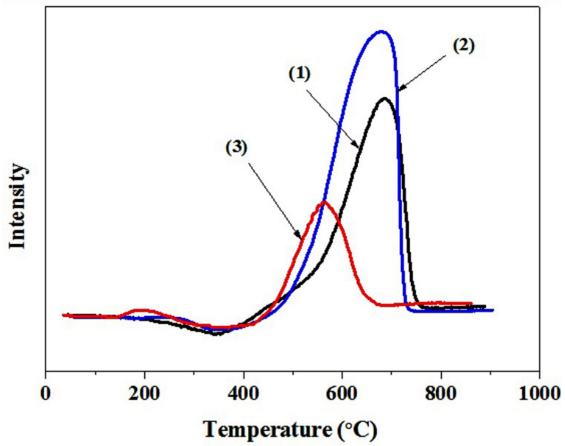

Fig. 16. TPO profiles of the spent catalysts with different potassium loadings (1) 15%Ni/1.5%K-Al_2O_3, (2) 15%Ni/3%K-Al_2O_3, (3) 15% Ni/6%K-Al_2O_3 catalysts.

4. Conclusions

The Ni/Al_2O_3 and the K_2O promoted Ni/Al_2O_3 catalysts were prepared and employed in CO_2 reforming of methane. The obtained results showed that the addition of potassium to the catalyst decreased the BET surface area and increased the pore diameter. The TPR results showed that the addition of a potassium promoter improved the catalyst reducibility. The catalytic activity increased dramatically and the coke formation decreased considerably by adding potassium to the catalyst during CRM. The textural properties of the $Ni/K-Al_2O_3$ catalysts with various Ni and K contents showed a decrease in specific surface area when K and Ni loadings were increased, due to partial blockage of the catalyst pores. The catalytic results demonstrated that the activity increased when the Ni loading increased because more accessible Ni active sites were provided for the reactants. The coke formation increased as the Ni content increased because of increases in catalyst particle size. The results showed that there is an optimum for potassium content where the catalyst showed the highest catalytic activity and the lowest carbon deposition.

Acknowledgment

The authors gratefully acknowledge the support from Iran National Science Foundation (INSF) and University of Kashan for supporting this work by Grant No. 158426/42.

5. References

[1] San José-Alonso D., Illán-Gómez M.J., Román-Martínez M.C., "K and Sr promoted Co alumina supported catalysts for the CO_2 reforming of methane", Catal. Today, 2011, 176: 187.

[2] Alipour Z., Rezaei M., Meshkani F., "Effect of alkaline earth promoters (MgO, CaO, and BaO) on the activity and coke formation of Ni catalysts supported on nanocrystalline Al_2O_3 in dry reforming of methane", J. Ind. Eng. Chem., 2014, 20: 2858.

[3] Seo H.O., Sim J.K., Kim K.D., Kim Y.D., Lim D.C., Kim S.H., "Carbon dioxide reforming of methane to synthesis gas over a TiO_2–Ni inverse catalyst", Appl. Catal. A. Gen., 2013, 451: 43.

[4] Newnham J., Mantri K., Amin M.H., Tardio J., Bhargava S.K., "Highly stable and active Ni-mesoporous alumina catalysts for dry reforming of methane", Int. J. Hydrogen Energy, 2012, 37: 1454.

[5] Xu L., Song H., Chou L., "Carbon dioxide reforming of methane over ordered mesoporous NiO–MgO–Al_2O_3 composite oxides", Appl. Cata.l B Environ.,2011, 108-109: 177.

[6] Arandiyan H., Li J., Ma L., Hashemnejad S.M., Mirzaei M.Z., Chen J., Chang H., Liu C., Wang C., Chen L., "Methane reforming to syngas over $LaNi_xFe_{1-x}O_3$ ($0 \le x \le 1$) mixed-oxide perovskites in the presence of CO_2 and O_2", J. Ind. Eng. Chem., 2012, 18: 2103.

[7] Meshkani F., Rezaei M., "Nickel catalyst supported on magnesium oxide with high surface area and plate-like shape: A highly stable and active catalyst in methane

reforming with carbon dioxide", Catal.Commun, 2011, 12: 1046.

[8] Hadian N., Rezaei M., Mosayebi Z., Meshkani F., "CO_2 reforming of methane over nickel catalysts supported on nanocrystalline $MgAl_2O_4$ with high surface area", J. Nat. Gas. Chem., 2012, 21: 200.

[9] Alipour Z., Rezaei M., Meshkani F., "Effects of support modifiers on the catalytic performance of Ni/Al_2O_3 catalyst in CO_2 reforming of methane", Fuel, 2014, 129: 197.

[10] Zanganeh R., Rezaei M., Zamaniyan A., "Dry reforming of methane to synthesis gas on NiO-MgO nanocrystalline solid solution catalysts", Int. J. Hydrogen Energy., 2013, 38: 3012.

[11] Arandiyan H., Peng Y., Liu C., Chang H., Li J., "Effects of noble metals doped on mesoporous LaAlNi mixed oxide catalyst and identification of carbon deposit for reforming CH_4 with CO_2", Technol. Biotechnol., 2013, 89: 372.

[12] Luo J., Yu Z., Ng C., Au C., "CO_2/CH_4 Reforming over Ni–La_2O_3/5A: An Investigation on Carbon Deposition and Reaction Steps", J. Catal., 2000, 194: 198-210.

[13] Wang S., Lu G., "A Comprehensive Study on Carbon Dioxide Reforming of Methane over Ni/γ -Al_2O_3 Catalysts", Ind. Eng. Chem. Res., 1999, 38: 2615.

[14] Asencios Y., Assaf E., "Combination of dry reforming and partial oxidation of methane on NiO–MgO–ZrO_2 catalyst: Effect of nickel content", Fuel Process. Technol., 2013, 106: 247.

[15] Hou Z., Yokota O., Tanaka T., Yashima T., "Characterization of Ca-promoted Ni/α-Al_2O_3 catalyst for CH_4 reforming with CO_2", Appl. Catal. A. Gen., 2003, 253: 381.

[16] Yu X., Wang N., Chu W., Liu M., "Carbon dioxide reforming of methane for syngas production over La-promoted NiMgAl catalysts derived from hydrotalcites", Chem. Eng. J., 2012, 209: 623.

[17] Meshkani F., Rezaei M., "Nanocrystalline MgO supported nickel-based bimetallic catalysts for carbon dioxide reforming of methane", Int. J. Hydrogen Energy, 2010, 35: 10295.

[18] Juan-Juan J., Román-Martínez M.C., Illán-Gómez M.J., "Effect of potassium content in the activity of K-promoted Ni/Al_2O_3 catalysts for the dry reforming of methane", Appl. Catal. A. Gen., 2006, 301: 9.

[19] Zhu J., Peng X., Yao L., Shen J., Tong D., Hu C., "The promoting effect of La, Mg, Co and Zn on the activity and stability of Ni/SiO_2 catalyst for CO_2 reforming of methane", Int. J. Hydrogen Energy, 2011, 36: 7094.

[20] Leofanti G., Padovan M., Tozzola G., Venturelli B., "Surface area and pore texture of catalysts", Catal. Today, 1998, 41: 207.

[21] Sutthiumporn K., Kawi S., "Promotional effect of alkaline earth over Ni-La_2O_3 catalyst for CO_2 reforming of CH_4: Role of surface oxygen species on H_2 production and carbon suppression", Int. J. Hydrogen Energy, 2011, 36: 14435.

[22] Roh H.S., Jun K.W., "Carbon Dioxide Reforming of Methane over Ni Catalysts Supported on Al_2O_3 Modified with La_2O_3, MgO, and CaO", Catal. Surv. Asia, 2008, 12: 239.

[23] García-Diéguez M., Herrera C., Larrubia M.Á., Alemany L.J., "CO_2-reforming of natural gas components over a highly stable and selective NiMg/Al_2O_3 nanocatalyst", Catal. Today, 2012, 197: 50.

[24] Wang S., Lu G., "Effects of promoters on catalytic activity and carbon deposition of Ni/γ-Al_2O_3 catalysts in CO_2 reforming of CH_4", J. Chem. Technol. Biotechnol., 2000, 75: 589.

[25] Ranjbar A., Rezaei M., "Preparation of nickel catalysts supported on $CaO.2Al_2O_3$ for methane reforming with carbon dioxide", Int. J. Hydrogen Energy, 2012, 37: 6356.